01 Feb 1974

Diffusion-Controlled Intrachain Reactions of Polymers. II Results for a Pair of Terminal Reactive Groups

Gerald Wilemski
Missouri University of Science and Technology, wilemski@mst.edu

Marshall Fixman

Recommended Citation

G. Wilemski and M. Fixman, "Diffusion-Controlled Intrachain Reactions of Polymers. II Results for a Pair of Terminal Reactive Groups," *Journal of Chemical Physics*, vol. 60, no. 3, pp. 878-890, American Institute of Physics (AIP), Feb 1974.
The definitive version is available at https://doi.org/10.1063/1.1681163

Diffusion-controlled intrachain reactions of polymers. II Results for a pair of terminal reactive groups*,†

Gerald Wilemski‡ and Marshall Fixman

Department of Chemistry, Yale University, New Haven, Connecticut 06520
(Received 18 September 1973)

The formulas and results of the preceding paper are used to calculate the rate of reaction between reactive groups attached to the ends of a polymer chain. Extensive numerical calculations have been made for both transient rate processes and steady state luminescence quenching. The results are restricted to chains in dilute solution, in either the free draining or nondraining limits and with no excluded volume forces present. A discussion of the qualitative effects of excluded volume forces on the results is included. The results suggest that experimental studies of these processes may be feasible.

I. INTRODUCTION

In the preceding article[1] (hereafter referred to as I) a general formalism has been used to describe the diffusion-controlled intramolecularly catalyzed reactions of special reactive sites incorporated in linear flexible chain molecules. The formalism requires that the reactive and catalytic sites be given specific, though not unique, locations along the chain backbone. From an experimental standpoint this is distressing because the synthesis of macromolecules with particular moieties at specific locations is apt to be difficult whereas obtaining a random distribution of sites ought to be much easier. For the theorist, however, the random distribution poses a problem because the formalism does not lend itself to the facile performance of the required random average. Presumably a Monte Carlo technique for sampling distributions and performing the average could be used. Even so, the presence of only a moderate number of catalytic sites would require the numerical evaluation of a large number of reduced Green's functions [cp. Eq. (I-94)] in order to compute the reactivity of even a single active site.

Fortunately there are some simple distributions which ought to be accessible both experimentally and computationally, and studies made for these distributions should yield information about the diffusive behavior of the chain that is potentially more useful than any obtained from results for random distributions. Perhaps the simplest of these consists of a pair of reactive groups attached to the ends of the chain. The results for this case depend directly on the relaxation of the end-to-end distance and may be a useful source of new information about low frequency relaxation behavior in chains. This special case is the subject of this article.

In order to utilize the existing formalism in a computational scheme only a specific choice of a reaction sink function must be made. This allows us to complete the evaluation of the reduced Green's function $D(t)$ and, hence, to calculate the quantities needed to perform the inversion of the Laplace transforms previously obtained. After this is done, several aspects of the numerical analysis will be reviewed. The remainder of this article will concentrate on the presentation of the numerical results and their interpretation in terms of the characteristics of the various models.

II. NUMERICAL CALCULATIONS

A. Choice of sink function

We immediately specialize to $m = 1$ in Eq. (I-94). Then

$$D(t) = \int d\mathbf{u}_1 d\mathbf{u}_2 \, s_1(\mathbf{u}_1) \, s_1(\mathbf{u}_2) \, D_{11}(\mathbf{u}_1, \mathbf{u}_2, t), \tag{1}$$

and we recall that $s_1(\mathbf{u})$ appears in Eq. (1) because of the use of the delta function in the evaluation of D_{11} via Eq. (I-89).

$$s_1(\mathbf{L}) = \int \delta(\mathbf{L} - \mathbf{u}) \, s_1(\mathbf{u}) \, d\mathbf{u} \, , \tag{2}$$

where

$$\mathbf{L} = \mathbf{r}_{N+1} - \mathbf{r}_1 \tag{3}$$

is the end-to-end vector of the polymer chain. For D_{11} in Eq. (1), Eqs. (I-112)–(I-116) and (I-136)–(I-138) give

$$\begin{aligned} D_{11}(\mathbf{u}_1, \mathbf{u}_2, t) = (2\pi L^2/3)^{-3} \, (1 - \rho_{\mathbf{L}}^2)^{-3/2} \\ \times \exp\{-3 \, [u_1^2 - 2\rho_{\mathbf{L}} \, \mathbf{u}_1 \cdot \mathbf{u}_2 + u_2^2] \\ \times [2 L^2 (1 - \rho_{\mathbf{L}}^2)]^{-1} \} \, . \end{aligned} \tag{4}$$

The time dependence of D_{11} resides in the autocorrelation function for $\mathbf{L}$ denoted here by $\rho_{\mathbf{L}}$.

The particular choice of sink function will be motivated by the need for computational convenience and by consideration of the grosser details of the reaction process. For example, a Gaussian form could be chosen in which case $D(t)$ would be given by another bivariate function. Perhaps the simplest choice which can be made is

$$s_1(\mathbf{L}) = \delta(\mathbf{L}) \, , \tag{5}$$

for which $D(t)$ is given as

$$D(t) = (2\pi L^2/3)^{-3} \, (1 - \rho_{\mathbf{L}}^2(t))^{-3/2} \, . \tag{6}$$

Equation (6) is appealing in that it does not depend on any parameters characterizing the reaction; hence the only new parameter needed in the development of this aspect of polymer theory would be k, the second order intrinsic rate constant. However, Eq. (6) possesses a strong singularity at $t = 0$ making it unsuitable for computational purposes since its Laplace transform would ostensibly diverge. A different choice for s is therefore indicated.

Another relatively simple choice is the Heaviside step function $H(x)$. However, its use produces a lengthy ex-

pression consisting of Gaussian functions, error functions, and integrals of the bivariate probability function which was deemed too cumbersome for numerical use in this initial, exploratory work.

The actual sink function used in this work stems from the employment of

$$s_1(\mathbf{L}) = \delta(\mathbf{L} - \mathbf{r}) . \tag{7}$$

However, the resulting $D(t)$ is still too singular to be useful. Therefore the $\mathbf{r}$ in one of the s's of Eq. (1) is averaged over a sphere of radius R. The other s is evaluated at $\mathbf{r} = 0$. This procedure is equivalent to the simultaneous use of Eq. (5) and the Heaviside function in Eq. (1), a somewhat "unbalanced" choice. However, an average over the second $\mathbf{r}$ would have negligible effect because $D(t)$ is a well behaved function of the second $\mathbf{r}$.

This procedure has the secondary effect of introducing an additional parameter R, the radius of the effective reaction volume, commonly found in other theories.[2] With this choice of sinks Eq. (1) gives

$$D(t) = (4\pi R^3/3)^{-1} \int d\mathbf{u}_1 d\mathbf{u}_2 H(R - u_1)\, \delta(\mathbf{u}_2) \times D_{11}(\mathbf{u}_1, \mathbf{u}_2, t) . \tag{8}$$

The integrals are easily done with the result

$$D(t) = (4\pi R^3/3)^{-1} (2\pi L^2/3)^{-3/2} K(t) , \tag{9}$$

where

$$K(t) = \mathrm{erf}[z(t)] - (2/\pi^{1/2}) z(t) \exp[-z^2(t)] , \tag{10}$$

$$\mathrm{erf}(x) = (2/\pi^{1/2}) \int_0^x \exp(-y^2) dy \tag{11}$$

$$z(t) = \gamma_R (1 - \rho_L^2(t))^{-1/2} , \tag{12}$$

and

$$\gamma_R = (3/2)^{1/2} (R/L) . \tag{13}$$

We note that the D's of Eqs. (6) and (9) become numerically equal as $t \to \infty$. That is, the equilibrium probability density for finding the ends in contact, multiplied by $4\pi R^3/3$, is approximately equal to the probability for finding the ends within a spherical volume of radius R:

$$(4\pi R^3/3) \langle 0 | \delta(\mathbf{L}) | \rho_{eq} \rangle \approx \langle 0 | H(L - R) | \rho_{eq} \rangle . \tag{14}$$

A brief inspection of the quantities in Eq. (14) shows that even for γ_R as high as 0.1 the approximate equality is satisfied very well.

B. Formulas resulting from the specific choice of sink function

First, recall that in I the probability $\phi(t)$ that the site has not yet reacted and the probability $\nu(t)$ that the unreacted ends are proximate were given as

$$\phi(t) = \sum_{i=1} \phi_i e^{-\theta_i t} , \tag{15}$$

$$\nu(t) = \sum_{i=1} \nu_i e^{-\theta_i t} . \tag{16}$$

We also have exactly from I

$$d\phi/dt = -k v_{eq} \nu(t) . \tag{17}$$

Then, the experimentally observable first order rate constant k_1 is obtained from Eq. (17) as

$$k_1 = -(d\phi/dt)/\phi(t) = k v_{eq} \nu(t)/\phi(t) . \tag{18}$$

Since, as will be seen, $\phi(t)$ is exceedingly well characterized by the first term of the sum in Eq. (15), Eq. (18) gives

$$k_1 = \theta_1 . \tag{19}$$

From Eq. (I-149) we can write

$$k_1 = \frac{k v_{eq}}{1 + (k/v_{eq}) \hat{H}(-k_1)} , \tag{20}$$

where $\hat{H}$ is the transform of $H(t)$ defined in Eq. (I-49) as

$$H(t) = D(t) - \lim_{t \to \infty} D(t) . \tag{21}$$

Next, a dimensionless "diffusion-reaction" parameter B may be introduced:

$$B = (kL^2/6D)(4\pi R^3/3)^{-1} . \tag{22}$$

The translational diffusion constant D of the macromolecule is given by[3,4]

$$D_{FD} = kT(N\beta)^{-1} \text{ (free draining)} \tag{23}$$

$$D_{ND} = 0.1928 kT (N^{1/2} b_0 \eta_0)^{-1} \text{ (nondraining).} \tag{24}$$

The factor $6D/L^2$ determines the time scale in terms of a dimensionless time variable τ:

$$\tau = (6D/L^2) t . \tag{25}$$

This time scale appears naturally in the harmonic spring model (see the Appendix of I), and was adopted throughout all of the calculations.

In terms of these scaled variables, Eqs. (9)–(14), (20)–(22), and (25) gives for k_1

$$k_1 L^2/6D = B K_\infty [1 + B\hat{K}_1(-k_1 L^2/6D)]^{-1} , \tag{26}$$

where

$$\hat{K}_1(\sigma) = \int_0^\infty e^{-\sigma\tau} K_1(\tau) d\tau , \tag{27}$$

$$K_1(\tau) = K(\tau) - K_\infty , \tag{28}$$

and

$$K_\infty = \lim_{\tau \to \infty} K(\tau) \tag{29}$$

$$= \mathrm{erf}(\gamma_R) - (2/\pi^{1/2}) \gamma_R \exp(-\gamma_R^2) . \tag{30}$$

Other quantities obtained in I can be readily expressed in terms of the scaled variables. For ν_1 and ϕ_1 of Eqs. (15) and (16) the equations read

$$\nu_1 = [1 + B\hat{K}_1(-k_1 L^2/6D) - (k_1 L^2/6D) B\hat{K}_1'(-k_1 L^2/6D)]^{-1} \tag{31}$$

and

$$\phi_1 = [1 + B\hat{K}_1(-k_1 L^2/6D)] \nu_1 , \tag{32}$$

where

$$\hat{K}_1'(\sigma) = -\int_0^\infty \tau e^{-\sigma\tau} K_1(\tau) d\tau . \tag{33}$$

For the integrals of $\nu(t)$ and $\phi(t)$ we have

$$\int_0^\infty \nu(\tau) d\tau = (BK_\infty)^{-1} \tag{34}$$

$$\int_0^\infty \phi(\tau) d\tau = [1 + B\hat{K}_1(0)][BK_\infty]^{-1} . \tag{35}$$

Finally, steady state luminescence quenching results can be calculated from Eq. (I-69) which now appears as

$$F^{-1}(\gamma+F)\,\Phi_{ss}=\frac{1+B\hat{K}_1(\omega)}{1+B\hat{K}_1(\omega)+BK_\infty\omega^{-1}}\,,$$

where

$$\omega=(\gamma+F)\,L^2(6D)^{-1}\,. \tag{36}$$

C. Numerical analysis

To perform the calculations, values of the functions $K(t)$ and $z(t)$ are required. Equation (10) defines $K(t)$. For the harmonic spring model it should readily be seen from the Appendix of I that

$$z(t)=\gamma_R\,[1-\exp(-6Dt/L^2)]^{-1/2}\,, \tag{37}$$

and for the segmented chain model, of course, Eq. (12) defines $z(t)$. Results from Secs. IV B and IV E of I enable us to write

$$\rho_L(t)=\left[\sum_{s=1}^{N}f_s^2\,(1+G_s)^{-1}\right]^{-1}\sum_{l=1}^{N}f_l^2(1+G_l)^{-1}\times\exp\left[-\Lambda_l(1+G_l)t\right]\,. \tag{38}$$

where Eq. (I-25) defines Λ_l. In order to give a more explicit expression for Λ_l we use Eq. (I-27) to calculate[3]

$$\langle 0\,|\,\mathbf{T}(\mathbf{r}_{ij})\,|\,\rho_{eq}\rangle=1(1-\delta_{ij})(6\pi^{3/2}\eta_0)^{-1}\times\left[\frac{1}{2}\sum_{l=1}^{N}f_l^2\,(1+G_l)^{-1}\right]^{-1/2}\,. \tag{39}$$

Thus, in the approximation that retains quadratic terms in the excluded volume potential we obtain

$$\Lambda_l=2kT\,\alpha_l^2\,[\beta^{-1}+2N^{1/2}\,((6\pi^3)^{1/2}b_0\eta_0)^{-1}E_{ll}]\,, \tag{40}$$

where

$$E_{kl}=b_0(12N)^{-1/2}\sum_{i\neq j}\sum Q_{ik}\,Q_{jl}\left[\sum_s f_s^2\,(1+G_s)^{-1}\right]^{-1/2}\,, \tag{41}$$

and the dependence of f_s on i and j is implicit. The E_{kl} have previously been defined by Horta and Fixman.[3]

For the $U=S^\alpha$ approximation we have

$$\rho_L(t)=\left(\sum_s f_s^2\right)^{-1}\sum_l f_l^2\exp(-\Lambda_l t) \tag{42}$$

which becomes

$$\rho_L(t)=(8/\pi^2)\sum_{l=1}l^{-2}\,[(-1)^l-1]^2\exp(-\Lambda_l t) \tag{43}$$

for $N\gg 1$. In this approximation we have the standard results[5]

$$\langle 0\,|\,\mathbf{T}(\mathbf{r}_{ij})\,|\,0\rangle=1(1-\delta_{ij})(6\pi^3|j-i|)^{-1/2}(\alpha b_0\eta_0)^{-1} \tag{44}$$

and

$$\Lambda_l=2kT\,\alpha_l^2\,[\beta^{-1}+(8N)^{1/2}[(6\pi^3)^{1/2}\,\alpha b_0\eta_0 l^2\pi^2]^{-1}\,I_1(l)]\,, \tag{45}$$

where $I_1(l)$ has been previously defined[5] as

$$I_1(l)=l^{1/2}\pi\,[l\pi\,C_2(l\pi)-(1/2)\,S_2(l\pi)]\,, \tag{46}$$

and the Fresnel integrals are given by

$$C_2(x)=(2\pi)^{-1/2}\int_0^x t^{-1/2}\cos(t)\,dt\,, \tag{47}$$

$$S_2(x)=(2\pi)^{-1/2}\int_0^x t^{-1/2}\sin(t)\,dt\,. \tag{48}$$

Calculations were performed using Eq. (43) for $\alpha=1$ (no excluded volume interaction) with Λ_l in its two well known limits: the freedraining limit,

$$\Lambda_l=3kT\,[l\pi/(\alpha N b_0)]^2\,\beta^{-1}\,, \tag{49}$$

and the nondraining limit,

$$\Lambda_l=12kT\,[(12\pi^3)^{1/2}\,(\alpha N^{1/2}\,b_0)^3\,\eta_0]^{-1}\,I_1(l)\,. \tag{50}$$

Equation (43) is very slowly convergent for small t, and computational facility is greatly enhanced by employment of the Euler–Maclaurin formula to evaluate the sum. With terms through third derivatives retained, the expression used for computation, in the free draining limit, is

$$(\pi^2/8)\,[1-\rho_L(t)]=\sum_{l=1}^{19}l^{-2}\,[(-1)^l-1]^2\,[1-e^{-l^2\tau_1}]+\tfrac{1}{2}(\tau_1\pi)^{1/2}\,[1-\mathrm{erf}(21\tau_1^{1/2})]+c_1[1-e^{-441\tau_1}]+\frac{1}{15}\left[28\tau_1^3+\frac{2}{21}\,\tau_1^2-\frac{2201}{(21)^3}\,\tau_1\right]e^{-441\tau_1}\,, \tag{51}$$

where

$$\tau_1=3kT\,[\pi/(Nb_0)]^2\beta^{-1}t \tag{52}$$

and

$$c_1=\frac{1}{42}+\frac{1}{882}+\frac{1}{3(21)^3}\left(1-\frac{4}{5(441)}\right)\,. \tag{53}$$

For $\tau_1=\infty$, this formula reproduces the values of $\pi^2/8$ to 9 significant figures, or better than 1 part in 10^9.

A similar expression for the nondraining limit is given by

$$(\pi^2/8)\,[1-\rho_L(t)]=\sum_{l=1}^{19}l^{-2}\,[(-1)^l-1]^2\,[1-e^{-\tau_2(2/\pi^{1/2})I_1(l)}]+I_a-I_b(s_0\,,\infty)+[c_1-\tfrac{1}{42}]\times[1-e^{-\tau_2(21\pi)^{1/2}(21\pi-1/2)}]+[c_2\tau_2+c_3\,\tau_2^2]e^{-\tau_2(21\pi)^{1/2}(21\pi-1/2)}\,, \tag{54}$$

where

$$I_a=\tfrac{1}{42}-I_b(21,\,s_0)\,, \tag{55}$$

$$I_b(x,y)=\tfrac{1}{2}\int_x^y ds\,s^{-2}\exp\left[-\tau_2(s\pi)^{1/2}\,(s\pi-\tfrac{1}{2})\right]\,, \tag{56}$$

and

$$\tau_2=6kT\,\pi^{1/2}\,[(12\pi^3)^{1/2}N^{3/2}b_0^3\,\eta_0]^{-1}\,t\,. \tag{57}$$

The c_i are listed in Table I. The values of the Fresnel integrals needed for the evaluation of $I_1(l)$ were calculated[6] for $l\leq 19$, but for $l\geq 21$ the asymptotic values, $S_2(\infty)=C_2(\infty)=\frac{1}{2}$, were used. Equation (54) is expected to be accurate to 9 decimal places for $\tau_2<10^{-6}$. When s_0 is chosen so that $\tau_2(s_0\pi)^{3/2}=1$, I_a will be given to 9 places by

$$I_a=(21\tau_2)^2\,\pi^3/8-\tau_2\,\pi\,\{(21\pi)^{1/2}+[2(21\pi)^{1/2}]^{-1}\}+\pi\,[c_4\,\tau_2^{2/3}+c_5\,\tau_2^{4/3}]\,. \tag{58}$$

With $\tau_2(s_0\pi)^{3/2}=1$, $I_b(s_0\,,\infty)$ can be transformed to read

$$I_b(s_0\,,\infty)=(\pi/2)\,\tau_2^{2/3}\int_1^\infty dx\,x^{-2}\times\exp\{-x^{3/2}\,[1-\tau_2^{2/3}(2x)^{-1}]\}\,. \tag{59}$$

Neglecting the $\tau_2^{2/3}$ term in the exponent which is always much less than one, this integral may be calculated as

TABLE I. Values of c_i, coefficients appearing in Eqs. (51), (54), and (58), displayed to the required precision.

i	c_i
1	0.0249792386
2	−0.014369581
3	0.7071
4	1.395207520
5	0.7097854

$$I_b = (\pi/2)\tau_2^{2/3}\left[e^{-1} - \Gamma(\tfrac{1}{3}) + \gamma(\tfrac{1}{3}, 1)\right] , \tag{60}$$

where Γ is the Gamma function and γ, the incomplete Gamma function, is defined as

$$\gamma(n,x) = \int_0^x e^{-y} y^{n-1}\, dy . \tag{61}$$

For $\tau_2 > 10^{-6}$ the sum in Eq. (43) was calculated explicitly, the upper limit being chosen as $s_0 = \pi^{-1}(20/\tau_2)^{2/3}$ for which any correction terms would be less than 10^{-10}. In case s_0 was determined to be in excess of 10 000, a new s_0 was computed from $s_0 = \tau_2^{-2/3}/\pi$ and the correction term $I_b(s_0, \infty)$ was added to the sum. Such precision in calculating these series was deemed necessary because of the sensitivity of $K(t)$ to small changes in $\rho_L(t)$, as can be seen by consulting Table II.

The primary feature of the numerical calculations is the computation of the various transform integrals. An effective upper limit t_∞ is easily found. The integrals over (t_∞, ∞) are then vanishingly small and can be neglected. The remaining integrals were computed by subdividing the interval $(0, t_\infty)$ into 16–27 subintervals depending on the behavior of the integrand, and the integral over each subinterval was computed with a 12 point Gauss–Legendre quadrature. Equation (26) was solved for k_1 using a simple iterative scheme which began with the guess $k_1 = 0$ on the right-hand side. In several instances δ_2 of Eqs. (15) and (16) was obtained from Eq. (I-153) which was rearranged into a form suitable for iterative solution. For this case the iteration was begun by setting δ_2 equal to the smallest nonzero chain relaxation frequency that is active in the reaction process. For both k_1 and δ_2, convergence to within 1% was usually obtained within 4–6 iterations. Knowledge of the coefficients arising in the expansion of $K(t)$ (obtained from the eigenfunction expansion of the Green's function) is needed to carry out the computation of δ_2. These coefficients, furthermore, determine the active chain relaxation frequencies in the reaction process; their calculation is presented in the Appendix.

The final point regarding the numerical calculations is that in terms of the dimensionless time variable τ, τ_1 and τ_2 of Eqs. (52) and (57) are given as

$$\tau_1 = (\pi^2/2)\tau , \tag{62a}$$

$$\tau_2 = (12^{1/2}\pi 0.1928)^{-1}\tau . \tag{62b}$$

III. RESULTS

A. Method of plotting

Henceforth, we abbreviate free draining and nondraining, respectively, as FD and ND.

Equations (13) and (22) give

$$B = \pi^{-1}(3/16)(3/2)^{1/2} k (DL\gamma_R^3)^{-1} . \tag{63}$$

Rate calculations were performed for $\gamma_R = 0.01$ and 0.05 with Eq. (26). Values of $k_1 L^2/6D$ are plotted versus $B\gamma_R^3$ in Fig. 1 for the various limits of the chain models used. Also included is the straight line[7] BK_∞ vs $B\gamma_R^3$ which is the maximum rate attainable and corresponds to the maintenance of an equilibrium distribution throughout the lifetime of the reaction. The effects of finite diffusivity are quite evident considering the large deviations from the predictions of the simple equilibrium theory.

Several aspects of the method of plotting are very important. First, each curve is valid only for a particular value of γ_R. Thus, along any particular curve, R and L are not independent parameters. Second, but most important, the results for the different models are plotted as if the D's appropriate to these models were equal for a given L. This is clearly not the case as can be seen by comparing Eqs. (23) and (24). However, because of the ambiguity associated with calculating D_{FD} for a given L, it is probably the most convenient way of presenting the results. Failure to appreciate this point can lead to very wrong conclusions regarding the relaxation behavior of these models. Thus, if it proved possible to obtain macromolecules such that

$$D_{ND} = D_{FD} \tag{64}$$

$$L_{ND} = L_{FD} , \tag{65}$$

the FD chain would have much higher relaxation rates, and its intrachain reactions would be much less limited by diffusion. However, a brief inspection of Eqs. (64) and (65), employing Eqs. (23) and (24) and with $L = N^{1/2} b_0$ and β given by Stokes' law as $\beta = 3\pi\eta_0 b_0$, will show that no physically self-consistent solution exists. Specifically this means that D_{FD} cannot equal D_{ND} for a given L, but has a correspondingly smaller value given by Eq. (23) (after some assignment for N, b_0 and/or β is made). The results of Fig. 1, then, are strictly comparable as predicted rates only if one were correlating independent

TABLE II. Values of $\rho_L(\tau)$ and $K(\tau)$ in the nondraining limit for selected values of τ; $\gamma_R = 0.01$.

τ	ρ_L	$K(\tau)$
2.397×10^{-9}	0.9999963	0.999994
2.187×10^{-8}	0.9999838	0.895778
1.133×10^{-7}	0.9999514	0.439854
3.106×10^{-7}	0.9999050	0.211571
1.133×10^{-6}	0.9997755	0.693223×10^{-1}
1.018×10^{-5}	0.9990380	0.884646×10^{-2}
3.503×10^{-4}	0.9901755	0.274301×10^{-3}
4.936×10^{-2}	0.7840707	0.314565×10^{-5}
5.046×10^{-1}	0.2666679	0.840215×10^{-6}
1.009	0.0876491	0.760959×10^{-6}
∞	0	0.752208×10^{-6}

TABLE III. Results for transient rate processes in nondraining chains without excluded volume forces; $\gamma_R = 0.01$. Listed are the decay constants δ_1 and δ_2, the expansion coefficients ϕ_1, ϕ_2, ν_1, and ν_2, and the quantities f_1^{ϕ} and κ. The former is the ratio of the integral of $\phi(t)$, with that function given by the lead term of its expansion, to the total integral of ϕ; the latter is the ratio of the diffusion-controlled (long time) rate constant to the maximum possible (equilibrium) value.

B	$\delta_1 L^2/6D$	ν_1	ϕ_1	f_1^{ϕ}	κ	$\delta_2 L^2/6D$	$\nu_2 \times 10^7$	$\phi_2 \times 10^8$
5.0×10^3	0.00373	0.992	1.00	1.00	0.992	4.4091	507	3.75
1.0×10^4	0.00741	0.985	1.00	1.00	0.985	4.4092	328	4.50
5.0×10^4	0.0350	0.929	1.00	1.00	0.929	4.4093	83.0	5.08
1.0×10^5	0.0653	0.868	1.00	1.00	0.868	4.4093	42.8	5.14
2.5×10^5	0.136	0.723	0.999	1.00	0.724	4.4094	17.5	5.17
5.0×10^5	0.213	0.565	0.996	1.00	0.567	4.4094	8.78	5.18
1.0×10^6	0.297	0.392	0.993	1.00	0.395	4.4094	4.41	5.19
2.5×10^6	0.388	0.204	0.987	0.999	0.206	4.4094	1.77	5.19
5.0×10^6	0.432	0.113	0.984	0.999	0.115	4.4094	0.883	5.19
1.0×10^7	0.458	0.0597	0.982	0.999	0.0608	4.4094	0.442	5.19
2.5×10^7	0.475	0.0247	0.980	0.999	0.0252	4.4094	0.177	5.19
5.0×10^7	0.480	0.0125	0.980	0.999	0.0128	4.4094	0.0884	5.19
1.0×10^8	0.484	0.00629	0.979	0.999	0.00643	4.4094	0.0442	5.19
5.0×10^8	0.486	0.00127	0.979	0.999	0.00129	4.4094	0.00884	5.19
∞	0.487	0	0.979	0.999	···	4.4094	0	5.19

measurements or estimates of D, L, and k. Having made these prefatory remarks we now undertake the interpretation of the results.

B. Rates for chains in the theta state

Numerical results for ND and FD chains with $\alpha = 1$ (no excluded volume forces) and $\gamma_R = 0.01$ are presented in Tables III and IV. Included in the results are the quantities f_1^{ϕ} and κ. The ratio of the integral of $\phi(t)$ with that function given by the first term of Eq. (15) to the total integral of ϕ given by Eq. (35) is denoted f_1^{ϕ}; κ is the ratio of the diffusion-controlled rate to the maximum rate under equilibrium conditions for a given value of B. This latter quantity then serves as a direct measure of the degree of deviation from the equilibrium rates. Another quantity, f_1^{ν}, can be defined by analogy with f_1^{ϕ}. However, this quantity is exactly identical to ϕ_1. The results show that the effect of the $i = 2$ term on the long time behavior is negligible. In almost all cases, the $i = 1$ term accounts for over 95% of the integral of ν and over 99% of the integral of ϕ. It appears possible in some cases for the sum $\phi_1 + \phi_2$ to exceed unity. This is solely the consequence of round off in preparing the tables. In the actual calculations the normalization was never exceeded.

Numerical results for $\gamma_R = 0.05$ and for the harmonic spring model have been presented elsewhere.[8] The trends in all of the results are very similar, and it is unnecessary to present additional tables because a convenient way of summarizing the results exists. Consider the expressions

$$k_1 L^2 (6D)^{-1} = BK_{\infty}(1 + BK_a)^{-1} , \tag{66}$$

$$\phi_1 = [1 + BK_a][1 + BK_a + k_1 L^2 (6D)^{-1} BK_a']^{-1} , \tag{67}$$

where

$$K_a = \hat{K}_1(-k_1^a L^2 (6D)^{-1}) \tag{68}$$

and

TABLE IV. Results for transient rate processes in free draining chains without excluded volume forces; $\gamma_R = 0.01$. Listed are the decay constants δ_1 and δ_2, the expansion coefficients ϕ_1, ϕ_2, ν_1, and ν_2, and the quantities f_1^{ϕ} and κ. The former is the ratio of the integral of $\phi(t)$, with that function given by the lead term of its expansion, to the total integral of ϕ; the latter is the ratio of the diffusion-controlled (long time) rate constant to the maximum possible (equilibrium) value.

B	$\delta_1 L^2/6D$	ν_1	ϕ_1	f_1^{ϕ}	κ	$\delta_2 L^2/6D$	$\nu_2 \times 10^3$	$\phi_2 \times 10^4$
5.0×10^3	0.00376	0.999	1.00	1.00	0.999	9.8733	0.375	0.00143
1.0×10^4	0.00750	0.997	1.00	1.00	0.997	9.8770	0.748	0.00569
5.0×10^4	0.0371	0.985	1.00	1.00	0.985	9.9063	3.67	0.139
1.0×10^5	0.0730	0.971	1.00	1.00	0.971	9.9423	7.17	0.542
5.0×10^5	0.327	0.867	0.998	1.00	0.869	10.206	29.9	11.0
1.0×10^6	0.577	0.762	0.995	1.00	0.766	10.483	48.1	34.5
2.5×10^6	1.06	0.552	0.981	0.999	0.563	11.070	68.0	116
5.0×10^6	1.46	0.373	0.962	0.996	0.388	11.606	65.4	212
1.0×10^7	1.79	0.223	0.940	0.994	0.238	12.079	48.5	302
2.5×10^7	2.06	0.101	0.918	0.991	0.110	12.487	25.0	375
5.0×10^7	2.17	0.0524	0.908	0.989	0.0577	12.651	13.6	407
1.0×10^8	2.23	0.0267	0.902	0.989	0.0296	12.739	7.12	422
5.0×10^8	2.28	0.00543	0.897	0.988	0.00605	12.813	1.47	434
∞	2.29	0	0.896	0.988	0	12.832	0	437

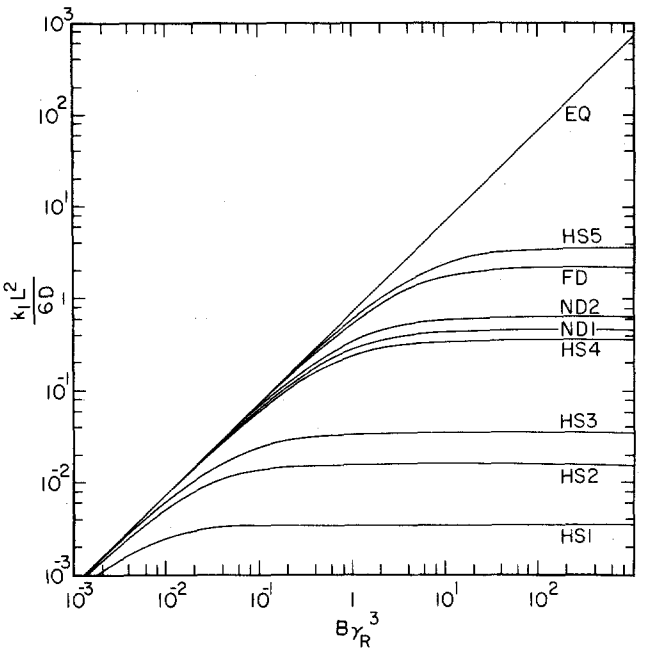

FIG. 1. Results for transient rate processes. EQ: Maximum rate under equilibrium conditions; FD: Free draining, no excluded volume forces, $\gamma_R = 0.01$; ND1: Non-draining, no excluded volume forces, $\gamma_R = 0.01$; ND2: Same as ND1, but $\gamma_R = 0.05$; HS1 through HS5: Harmonic spring model, $\xi = 1, 4.4082, \pi^2, 100, 1000$, respectively, and $\gamma_R = 0.01$.

$$K_a' = -\hat{K}_1'(-k_1^a L^2(6D)^{-1}) , \tag{69}$$

and k_1^a is the solution to Eq. (26) for $k = \infty (B = \infty)$. (A similar expression for ν_1 can readily be written down.) With the limiting values K_∞, K_a and K_a' appropriate for the different models and limits, these expressions are capable of reproducing the numerical results with very high accuracy over the entire range of B. None of the quantities calculated in this way deviated by more than 3.5% from the more precisely calculated quantities. Typically, the deviation was less than 1% with the largest deviations obtained for ν_1 in FD chains. Considering the approximate nature of the more precise calculations, this simplification is numerically inconsequential. The values of K_∞, K_a, and K_a' are listed in Table V.

Now let us compare the rates for the FD and ND chains for a given L. In order to make a definite comparision let us again put $\beta = 3\pi\eta_0 b_0$, then Eqs. (23) and (24) give

$$D_{ND} = (0.1928)(3\pi) N^{1/2} D_{FD} , \tag{70}$$

and with Eq. (63), the B's are related by

$$B_{FD} = (0.1928)(3\pi) N^{1/2} B_{ND} . \tag{71}$$

Thus, B_{FD} is arbitrary to the extent that N (or b_0) is. With Eqs. (66), (70) and (71) the ratio of k_1 for the FD chain to that for the ND chain may be approximately expressed as

$$\frac{k_1^{FD}}{k_1^{ND}} = \frac{1 + B_{ND} K_a^{ND}}{1 + (0.1928)(3\pi) N^{1/2} B_{ND} K_a^{FD}} . \tag{72}$$

Using Table V to evaluate Eq. (72) it can be seen that k_1^{FD} will equal or exceed k_1^{ND} *only* for $N \lesssim 7$ when $\gamma_R = 0.01$ and for $N \lesssim 4$ when $\gamma_R = 0.05$. So we see that for physically reasonable values of N the ND chain always exhibits larger rates than the FD chain, and we therefore conclude that the ND chain has a higher diffusive response than the FD chain for a given L. Of course, Eq. (72) always approaches unity for very small B in which case the reaction is no longer diffusion-controlled, and the chain dynamics are therefore unimportant.

It should be mentioned that the theory has dubious applicability when N is as small as the values mentioned above, particularly for the nondraining limit. Realistic predictions for such small chains would require a different theoretical treatment of the chain dynamics, and the rates would probably not be diffusion-controlled unless the chains were very stiff.

Next, let us consider the R dependence of the rates. Note that a vertical translation between curves for different γ_R represents a fivefold change in R since only two values of γ_R, 0.01 and 0.05, were used in the calculations. For the FD chain this increase has only a slight effect on k_1. The increases in $k_1 L^2/6D$ are less than 4.2% over the entire range of abscissa. Consequently these results have not been included in Fig 1. For the ND chain the changes are more pronounced with increases of up to 42% occurring. The increased reaction volume must act as an additional advantage for the relatively mobile ND chain whereas it does not appreciably enhance the reactivity of the more slowly relaxing FD chain.

Regarding the L dependence at constant R, for the ND chain the product $D_{ND}L$ is independent of L (or N), so the effect of increasing L at constant R is shown by jumping vertically to a curve characterized by smaller γ_R. For the FD chain, the product $D_{FD}L$ is not independent of N so increasing L also increases $B_{FD}\gamma_R^3$. In both cases increasing L reduces the reaction rate. It is instructive to compare the relative decreases in rates incurred by the FD and ND chains when L is increased by a factor of 5 and R is held constant. Using Eqs. (23), (24), (66), (70), and (71) it is readily established that in this case the FD chain always suffers a proportionately greater decrease in rate than the ND chains for any given reference value of B_{ND}. It seems reasonable to suppose that this behavior will, in general, be true for

TABLE V. Values of K_∞, K_a, and K_a'.

γ_R	0.01	0.05
$K_\infty (\times 10^7)$	7.522	938.9
Nondraining		
$K_a (\times 10^6)$	1.546	139.7
$K_a' (\times 10^8)$	6.824	918.95
Free draining		
$K_a (\times 10^7)$	3.288	393.8
$K_a' (\times 10^8)$	1.668	212.2
Harmonic spring		
$K_a (\times 10^4)$	2.002	...
$K_a' (\times 10^6)$	2.559	...

any increase in L. Thus the implication is found that because of its higher diffusive response the ND chain is better able to offset the adverse effect on relaxation rates arising from increased chain size than is the FD chain.

Other interesting results remain to be mentioned. One particularly useful estimate which can be made is of the size of k which must obtain in order for significant departure from equilibrium rates to occur. For the ND chain k_1 deviates from the equilibrium prediction by about 7% at $B\gamma_R^3 = 0.05$ when $\gamma_R = 0.01$. The deviation increases to 13% at $B\gamma_R^3 = 10^{-1}$. For this latter case, with $T = 300\,^\circ$K, $\eta_0 = 1$ cp, Eqs. (24) and (63) give $k \approx 1.1 \times 10^{-12}$ cm^3/sec or about 10^9 liters (mole-sec)$^{-1}$ which is about an order of magnitude smaller than values which are typically quoted[9] for reactions involving small molecules. The presence of excluded volume forces might be expected to lower this threshold by at least another order of magnitude. For comparison, the FD chain shows a 13% deviation at $B\gamma_R^3 = 0.5$ Eqs. (23) and (63) with $\beta = 3\pi\eta_0 b_0$ give

$$k \approx N^{-1/2}\, 3 \times 10^{-12} \text{ cm}^3/\text{sec}$$

for the same T and η_0 as above. Even for $N = 100$, this value is about 27% of that for the ND chain.

A more relevant quantity for experiment is the first order rate constant k_1 defined in Eq. (18). Using Eq. (66), the approximate value of k_1 for any given fractional deviation, say $100x$%, from the equilibrium rate may be given as

$$k_1 = x(6D/L^2)(K_\infty/K_a) \,. \tag{73}$$

Values of k_1 are listed in Table VI for a 10% deviation from the equilibrium rate.

Let us now define a quantity k_2,

$$k_2 = k_1/v_{eq} \,, \tag{74}$$

which is the long time value of the second order rate constant that would be "observed" if an independent measurement or estimate of v_{eq} were available. Using Eqs. (63) and (66), Eq. (74) gives

$$k_2 = \frac{4\pi DR}{(4\pi DR/k) + (3K_a/4\gamma_R^2)} \,, \tag{75}$$

and also

$$k_2 = \frac{4\pi DL}{(4\pi DL/k) + (\frac{3}{2})^{3/2}(K_a/2\gamma_R^3)} \,. \tag{76}$$

Equation (75) has the form obtained in several theories[10] for bimolecular reactions of small molecules. The difference is that in those theories unity appears instead of the term $3K_a/4\gamma_R^2$. The term $3K_a/4\gamma_R^2$ is considerably smaller than unity, and this enables diffusion-controlled effects to be produced for smaller values of k.

There are two different ways of regarding the parameter γ_R. One way is to deprive R of physical significance and pick γ_R so that the agreement between Eqs. (6) and (9) for $D(t)$ is made over the largest range of t, while the singularity is still smoothed over. Obviously, choosing γ_R to be ever smaller, but nonzero, will accomplish this, but then no criterion exists for determining how small γ_R is to be made. Figure 2 shows plots of $K(\tau)/\gamma_R^3$ for the two values of γ_R compared with Eq. (6) for the ND chain. Recalling that $D_{ND}L$ is independent of L (or N), this view of γ_R also implies that k_2 for the ND chain would be independent of L since the factor K_a/γ_R^3 would be a constant in Eq. (76). The alternative view has been employed implicitly throughout this discussion. The parameter R is interpreted as some kind of effective collision radius within which the reaction can occur. In this interpretation, k_2 of Eq. (76) is predicted to have an L dependence since γ_R and K_a are now functions of (R/L). The former view also predicts that for the ND chain the conditional probability density $\eta(t)$ for finding the ends in proximity depends on L only through v_{eq} at long times since

$$\eta(t) = v_{eq}\,\nu(t)/\phi(t) \,,$$

and by Eqs. (18) and (74)

$$\eta = k_2 v_{eq}/k \,.$$

Since increasing L slows down the chain relaxation as well as lowers v_{eq}, η might be expected to exhibit an additional L dependence through k_2. Thus the latter view of γ_R and R seems preferable.

C. Qualitative results for chains with excluded volume forces

Before proceeding further, a brief discussion on the effect of different time scales is appropriate. Consider

$$\hat{K}_1^s(\sigma) = \int_0^\infty e^{-\sigma\tau} K_1(\xi\tau)\, d\tau \,, \tag{77}$$

where ξ is a scaling factor. The time dependence of $K_1(\tau)$ could be that appropriate to any of the various models and limits we have discussed. In terms of $K_1(\tau)$ Eq. (77) may be rewritten as

$$\hat{K}_1^s(\sigma) = \xi^{-1}\hat{K}_1(\sigma\xi^{-1}) = \xi^{-1}\int_0^\infty e^{-\sigma\xi^{-1}\tau} K_1(\tau)\, d\tau \,. \tag{78}$$

TABLE VI. Examples of the smallest first order rate constants expected to be characteristic of a diffusion-controlled reaction; calculated from Eq. (73) with $T = 300\,^\circ$K and $\eta_0 = 1$ cp. These values deviate from the equilibrium rate constants by 10%. For a deviation of 1% the values would be one order of magnitude smaller. The maximum diffusion-controlled rate ($B = \infty$) is one order of magnitude larger than these values. Note for the FD chain that the reported quantity is $N^{1/2}k_1$.

L(Å)	R(Å)	Nondraining k_1(sec^{-1})	Free draining $N^{1/2}k_1$ (sec^{-1})
100	4.08	3.22×10^5	6.29×10^5
100	0.82	2.33×10^5	6.03×10^5
200	8.16	4.02×10^4	7.86×10^4
200	1.63	2.91×10^4	7.54×10^4
300	12.25	1.19×10^4	2.33×10^4
300	2.45	8.63×10^3	2.23×10^4
400	16.33	5.03×10^3	9.82×10^3
400	3.27	3.64×10^3	9.42×10^3
500	20.41	2.58×10^3	5.03×10^3
500	4.08	1.86×10^3	4.83×10^3
750	30.62	7.63×10^2	1.49×10^3
750	6.12	5.53×10^2	1.43×10^3
1000	40.82	3.22×10^2	6.29×10^2
1000	8.16	2.33×10^2	6.03×10^2

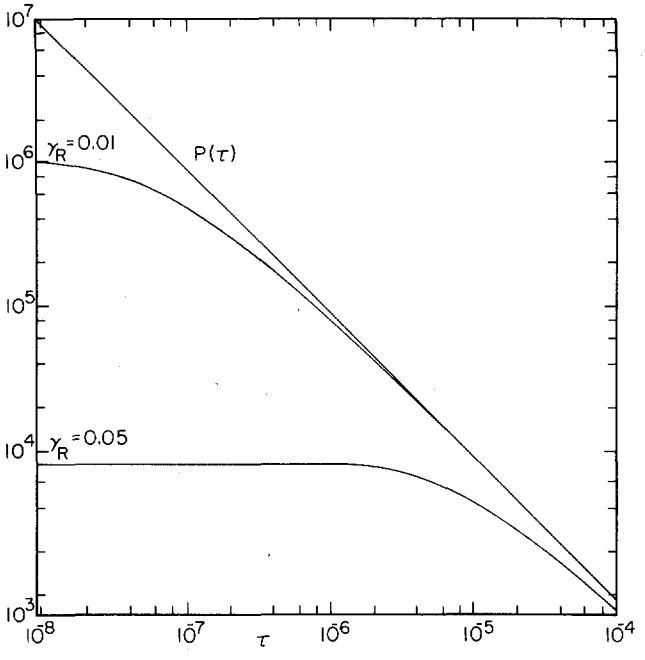

FIG. 2. The function $K(\tau)/\gamma_R^3$ for $\gamma_R = 0.01$ and 0.05 compared with $P(\tau) = [4/(3\pi^{1/2})]\,[1-\rho_L^2(\tau)]^{-3/2}$.

Equation (78), of course, just represents the scaling property of the Laplace transform. With the fundamental time scale set by D and L of the unscaled system ($\xi = 1$), the rate for the scaled system, k_1^s, for a value of B is obtainable from the rate, k_1', for B/ξ in the unscaled system as

$$k_1^s = \xi k_1' \,. \tag{79}$$

Equation (79) follows directly from Eqs. (26) and (78).

For $\xi < 1$, the resulting rates are scaled down relative to the unscaled, that is,

$$k_1^s \leq k_1 \,, \tag{80}$$

where k_1 is the rate in the unscaled system computed for the *same* B as k_1^s. To see this, note that $k_1' > k_1$ and that the maximum value k_1' can attain for a given B and ξ is $k_1' = k_1/\xi$. This value will be reached when both k_1' and k_1 are specified by the linear relation which holds under equilibrium conditions: $k_1 L^2/6D = BK_\infty$. Otherwise, we have $k_1' < k_1/\xi$. Hence, $k_1' \leq k_1/\xi$, and using this result with Eq. (79) we obtain Eq. (80). Similar reasoning holds for $\xi > 1$, implying

$$k_1^s \geq k_1 \,, \tag{81}$$

so that the curves would be displaced upward.

We are now able to discuss the qualitative effects of excluded volume forces on the reaction rates. First, consider the $U = S^\alpha$ approximation. For $N \gg 1$ in the nondraining limit, Eq. (50) gives

$$\Lambda_l = \alpha^{-3}(\lambda_l/2) \,, \tag{82}$$

where λ_l is the Zimm–Hearst[11] relaxation frequency. The factor α^{-3} acts as the scaling factor ξ introduced in Eq. (77). Since

$$\alpha^{-3} \leq 1 \,, \tag{83}$$

the rates in the presence of excluded volume forces will be diminished. In this approximation the chain relaxation has been retarded relative to the unperturbed state. Next, we consider the approximation in which the excluded volume potential is expanded through quadratic terms in the boson representation. From Eq. (38) the relevant relaxation frequencies are seen to be the $\Lambda_l \times (1+G_l)$. Earlier results of Fixman[12] give

$$\begin{aligned} &\Lambda_l(1+G_l) = \Lambda_l \,, \quad l = 1 \,; \\ &\Lambda_l(1+G_l) = \alpha^2 \Lambda_l (1 - \alpha^{-5} z g_l) \,, \quad l > 1 \,. \end{aligned} \tag{84}$$

Since

$$\Lambda_l(1+G_l) > 0 \,, \tag{85}$$

Eq. (84) and (85) give

$$1 - \alpha^{-5} z g_l \leq 1 \,. \tag{86}$$

In the ND limit Eqs. (40) and (50) give

$$\alpha^2 \Lambda_l = 2^{-3/2} \lambda_l \, l^2 \pi^2 E_{ll}/I_1(l) \,, \tag{87}$$

and we have also

$$\lim_{\alpha \to 1} 2^{-1/2} l^2 \pi^2 E_{ll}/I_1(l) = 1 \,. \tag{88}$$

Since the E_{ll} are decreasing functions of α,

$$\alpha^2 \Lambda_l < \lambda_l/2 \,. \tag{89}$$

Then, Eqs. (84), (86), and (89) give

$$\Lambda_l(1+G_l) < \lambda_l/2 \,, \tag{90}$$

and we can write

$$\Lambda_l(1+G_l) = \xi_l(\alpha)\lambda_l/2 \,. \tag{91}$$

Since the g_l vanish for large l,

$$\Lambda_l(1+G_l) \to \alpha^2 \Lambda_l \,, \quad l \gg 1 \,; \tag{92}$$

and even in this approximation the highest relaxation frequencies are still predicted by Eq. (87) to show an excluded volume effect through E_{ll}. Equation (91) shows that a single scaling factor is now insufficient, and the results of Eqs. (77)–(81) do not apply exactly. All of the $\xi_l(\alpha)$ are less than 1, however, so this approximation also predicts a retardation of the chain relaxation and a corresponding diminishment of the reaction rates. The situation is somewhat more complicated because the coefficients in Eq. (38) are also seen to depend on the excluded volume forces through the G_l. As the strength of the interaction is increased the contribution of the first term will dominate the sum, and the time dependence might well be characterized as

$$\rho_L(t) \sim e^{-\Lambda_1(t)} \,. \tag{93}$$

This is, of course, formally the same time dependence as that of the simple model. Calculations were made with Eq. (93) in the FD and ND limits but with Λ_1 evaluated from Eqs. (49) and (50) with $\alpha = 1$, which corresponds to scale factors of $\xi = \pi^2$ and 4.408, respectively, relative to the harmonic spring (HS) model as discussed below. Even so, the rates, reported in Fig. 1 as curves HS3 and HS2, show a large decrease relative to those for the unperturbed chains.

If the interpretations made on the basis of these approximate ways of including excluded volume forces are valid, it seems plausible that the relaxation of the nondraining chain can be significantly retarded by the excluded volume forces so that the predicted reaction rates could approach or even become smaller than those calculated for the unperturbed free draining chain. These interpretations agree with Verdier's[13] observations regarding the dynamics of chains on lattices. Namely, the excluded volume effect and the hydrodynamic interaction have opposing effects on the chain relaxation, and the unperturbed free draining chain might be appropriate in the simultaneous presence of these two forces.

D. Harmonic spring model

The actual calculations shown in Fig. 1 were made with the time scale, $\xi = 1$, set by the diffusion constant characteristic of a macromolecule rather than that characteristic of small molecules. These results were scaled with $\xi = 100$ and 1000 in the manner described by Eqs. (77)–(81), in order to get results appropriate to the diffusion of small molecules coupled by a spring. We have already noted above that the HS results scaled for $\xi = \pi^2$ and 4.408 represent approximately the limit of very large excluded volume forces in free draining and non-draining chains, respectively.

The two cases, $\xi = 100$ and $\xi = 1000$, correspond to systems for which the small molecule diffusion constant is 100 and 1000 times as large as the macromolecular diffusion constant. The curves for these two cases lie near, respectively, the curves for unperturbed nondraining and free draining chains. Since D_{ND} is usually at least an order of magnitude larger than D_{FD} and since $100D_{FD}$ and $1000D_{FD}$ are approximately the right order of magnitude for diffusion constants of small molecules, the results seem qualitatively in accord with the presemption that the average force on the ends arising from the internal segments is crudely approximated by the harmonic spring.

E. Mean first passage time for end-to-end contact

Following Montroll and Shuler[14] we may define a mean first passage time, $\tau_m(k)$, for the first reactive encounter between the chain ends:

$$\tau_m(k) = -\int_0^\infty t(d\phi/dt)\,dt \ . \tag{94}$$

Recalling Eq. (17) and using the properties of the Laplace transform, this expression can be evaluated as

$$\tau_m = -\left.\frac{ds\hat{\phi}(s)}{ds}\right|_{s=0} = -kv_{eq}\left.\frac{d\hat{\nu}(s)}{ds}\right|_{s=0} \ . \tag{95}$$

With Eq. (I-52) and/or Eq. (I-51), τ_m is approximately given as

$$\tau_m(k) = [1 + (k/v_{eq})\hat{H}(0)]\,[kv_{eq}]^{-1} \ , \tag{96}$$

and in terms of the function $K(t)$ and the scaled variables used in the numerical calculations Eq. (96) gives

$$\tau_m 6DL^{-2} = [1 + B\hat{K}_1(0)]\,[BK_\infty]^{-1} \tag{97}$$

which should be compared with Eq. (35). Equations (15) and (94) may also be used to evaluate τ_m with the result

$$\tau_m = \sum_i \phi_i \delta_i^{-1} \ . \tag{98}$$

The $i = 1$ term dominates the sum, and we note that values of $\phi_1/(\delta_1\tau_m)$ with τ_m given by Eq. (97) have already been presented in Tables III and IV as the quantity f_1°. The agreement obtained by using only the $i = 1$ term is notable.

The mean first passage time for *first* contacts between ends is obtained from Eq. (97) upon taking the limit $B \to \infty (k \to \infty)$. In this limit $\nu = 0$ and ϕ constitutes an approximate solution to the mean first passage time problem of first contacts between the chain ends, since $(-d\phi/dt)dt$ will give the probability that the ends first touch in the interval dt.

F. Results for luminescence quenching

In view of the lengthy presentation of results for the transient rates, little additional discussion seems necessary for the luminescence quenching results. Representative results are presented in Tables VII–IX. As an illustration, results for $B\gamma_R^3 = 5$ are plotted in Fig. 3. As is the case above, no direct comparison between the results for the ND and FD chains can be made from the figures because the time scales which are set by D for a given L are different. Therefore, some numerical comparisions may be illuminating. Equation (71) relates (approximately) the different B's. Equation (70) will enable us to relate the values of $\gamma + F$ as they are scaled in the two systems. Let

$$(\gamma + F)_{ND} = (\gamma + F)\,L^2(6D_{ND})^{-1} \ , \tag{99}$$

and

$$(\gamma + F)_{FD} = (\gamma + F)\,L^2(6D_{FD})^{-1} \ , \tag{100}$$

then, Eq. (70) gives

$$(\gamma + F)_{FD} = (0.1928)(3\pi)N^{1/2}(\gamma + F)_{ND} \ . \tag{101}$$

The quantity $0.1928(3\pi)N^{1/2}$ also relates the two B's of Eq. (71). For $N = 121$ this quantity is approximately equal to 20, and for $N = 750$ it is approximately 50. From Table VII for $B = 5\times10^5$ and $(\gamma + F)_{ND} = 0.5$ the fraction of molecules in the excited state relative to the unquenched system is predicted to be 0.698 for the ND chain for any N (γ_R is fixed at 0.01). For the FD chain with $N = 121$, $B = 1\times10^7$ and $(\gamma + F)_{FD} = 10$, Table VIII gives the corresponding value of 0.815. With $T = 300$ °K, $\eta_0 = 1$ cp, and $L = 100$ Å this value of $(\gamma + F)_{ND}$ gives approximately $(\gamma + F)^{-1} = 4\times10^{-6}$ sec. Again, for the ND chain from Table VII for $B = 1\times10^6$ and $(\gamma + F)_{ND} = 1.0$ the fraction is 0.765. For the FD chain, this time for $N = 750$, with $B = 5\times10^7$ and $(\gamma + F)_{FD} = 50.0$, Table VIII gives 0.925 for the fraction. In this case for $L = 100$ Å we have $(\gamma + F)^{-1} = 2\times10^{-6}$ sec., and for $L = 250$ Å we obtain approximately 3×10^{-5} sec. The ND chain gives consistently more quenching, and the lifetimes are not physically unreasonable for luminescent species.

In general, all of the same trends can be found in these results as were found above. The ND chain, which has a higher diffusive response, shows proportionately more quenching for given values of k, R, L, and $\gamma + F$. The excluded volume effect lowers the diffusive response; the hydrodynamic interaction raises it. The

TABLE VII. Luminescence quenching results. Values of $\Phi_{ss}F^{-1}$ $(\gamma+F)$ for nondraining chains without excluded volume forces; $\gamma_R = 0.01$.

$B=$	5×10^4	1×10^5	5×10^5	1×10^6	5×10^6	1×10^7	5×10^7	1×10^8	5×10^8	∞
$(\gamma+F)L^2(6D)^{-1}$										
1.0×10^{-2}	0.222	0.133	0.0446	0.0324	0.0223	0.0210	0.0200	0.0199	0.0198	0.0197
3.0×10^{-2}	0.462	0.315	0.123	0.0911	0.0640	0.0605	0.0577	0.0573	0.0570	0.0569
5.0×10^{-2}	0.588	0.433	0.189	0.143	0.102	0.0967	0.0924	0.0918	0.0914	0.0913
7.0×10^{-2}	0.667	0.517	0.246	0.189	0.137	0.130	0.124	0.124	0.123	0.123
1.0×10^{-1}	0.741	0.605	0.318	0.250	0.185	0.176	0.169	0.168	0.167	0.167
2.5×10^{-1}	0.877	0.793	0.537	0.453	0.360	0.346	0.335	0.333	0.332	0.332
5.0×10^{-1}	0.935	0.884	0.698	0.623	0.528	0.513	0.500	0.498	0.497	0.497
7.5×10^{-1}	0.955	0.920	0.775	0.710	0.624	0.609	0.596	0.595	0.593	0.593
1.0	0.966	0.938	0.821	0.765	0.686	0.672	0.661	0.659	0.658	0.657
4.0	0.991	0.984	0.947	0.926	0.892	0.886	0.880	0.879	0.878	0.878
7.0	0.995	0.991	0.968	0.955	0.932	0.927	0.923	0.922	0.922	0.922
1.0×10^{1}	0.996	0.993	0.978	0.968	0.951	0.948	0.945	0.945	0.944	0.944
3.0×10^{1}	0.999	0.998	0.992	0.988	0.981	0.980	0.979	0.978	0.978	0.978
5.0×10^{1}	0.999	0.999	0.995	0.993	0.988	0.987	0.987	0.986	0.986	0.986
1.0×10^{2}	1	0.999	0.997	0.996	0.994	0.993	0.993	0.992	0.992	0.992

maximum quenching that could be obtained is that predicted by the equilibrium theory from the equation

$$\Phi_{ss}^{eq} = F(\gamma+F)^{-1}\left[1+kv_{eq}(\gamma+F)^{-1}\right]^{-1} = F(\gamma+F)^{-1}\left[1+BK_\infty 6DL^{-2}(\gamma+F)^{-1}\right]^{-1} . \quad (102)$$

Values calculated with Eq. (102) are recorded in Table IX. There is sufficient deviation between these results and those for the chain models to permit a clear choice in any experimental test.

Although extensive caluclations have been made[8] with Eq. (36) for Φ_{ss}, there exists an alternative and simpler way of obtaining these results. If Eqs. (I-68) and (15) are used to calculate Φ_{ss}, the resulting equation reads

$$\Phi_{ss}F^{-1}(\gamma+F) = \sum_i \phi_i\left[1+\delta_i(\gamma+F)^{-1}\right]^{-1} . \quad (103)$$

The first term dominates the sum, and values calculated from the $i=1$ term of Eq. (103) for ND and FD chains with $\gamma_R = 0.01$ are in good to excellent agreement with those in Tables VII and VIII. The agreement is excellent for the ND chain and good for the FD chain. The only significant discrepancy, but never more than 10%, occurs in the FD results for large values of both B and $(\gamma+F)L^2/6D$, and can be attributed to the deviation of ϕ_1 from unity. The inclusion of the $i=2$ term would lead to improvements of several percent in this case. Since δ_1 and ϕ_1 are easily calculated with high accuracy by using the asymptotic values of $\hat{K}_1$ and $\hat{K}_1'$, K_a and K_a', Φ_{ss} can be calculated straightforwardly with the first term of Eq. (103) for any values of k and $\gamma+F$.

For an instantaneous pulse of light at $t=0$ which excites a fraction f of the potentially luminescent sites, the decay law is readily obtained in the form

$$\Phi(t) = f\phi(t)\exp(-\gamma t) . \quad (104)$$

The long time dependence goes as $\exp[-(\delta_1+\gamma)t]$, and perusal of the results shows that δ_1 and γ can be found comparable in magnitude over a significant range. It thus appears possible to find conditions under which the transient behavior with intrachain quenching differs sig-

TABLE VIII. Luminescence quenching results. Values of $\Phi_{ss}F^{-1}$ $(\gamma+F)$ for free draining chains without excluded volume forces; $\gamma_R = 0.01$.

$B=$	5×10^4	1×10^5	5×10^5	1×10^6	5×10^6	1×10^7	5×10^7	1×10^8	5×10^8	∞
$(\gamma+F)L^2(6D)^{-1}$										
1.0×10^{-2}	0.213	0.120	0.0296	0.0170	0.00658	0.00526	0.00421	0.00408	0.00397	0.00395
3.0×10^{-2}	0.447	0.291	0.0840	0.0492	0.0195	0.0156	0.0125	0.0121	0.0118	0.0117
5.0×10^{-2}	0.574	0.406	0.132	0.0794	0.0320	0.0257	0.0207	0.0200	0.0195	0.0194
7.0×10^{-2}	0.654	0.489	0.176	0.108	0.0442	0.0356	0.0286	0.0277	0.0270	0.0269
1.0×10^{-1}	0.730	0.578	0.234	0.147	0.0620	0.0501	0.0404	0.0392	0.0382	0.0380
2.5×10^{-1}	0.871	0.774	0.433	0.301	0.141	0.116	0.0945	0.0918	0.0896	0.0890
5.0×10^{-1}	0.931	0.872	0.604	0.462	0.246	0.207	0.172	0.167	0.163	0.163
7.5×10^{-1}	0.953	0.911	0.695	0.562	0.327	0.278	0.234	0.228	0.224	0.222
1.0	0.964	0.932	0.752	0.630	0.391	0.337	0.287	0.280	0.275	0.273
4.0	0.991	0.982	0.923	0.870	0.709	0.656	0.597	0.588	0.581	0.579
7.0	0.995	0.990	0.954	0.920	0.800	0.754	0.699	0.690	0.683	0.681
1.0×10^{1}	0.996	0.993	0.967	0.942	0.852	0.815	0.770	0.762	0.756	0.755
3.0×10^{1}	0.999	0.998	0.989	0.979	0.938	0.918	0.888	0.883	0.879	0.877
5.0×10^{1}	0.999	0.999	0.993	0.987	0.960	0.946	0.925	0.921	0.917	0.916
1.0×10^{2}	1	0.999	0.996	0.993	0.978	0.968	0.952	0.949	0.946	0.945
4.0×10^{2}	1	1	0.999	0.998	0.994	0.990	0.984	0.982	0.981	0.980

TABLE IX. Luminescence quenching results. Values of $\Phi_{ss}^{eq} F^{-1}$ $(\gamma+F)$, the equilibrium results corresponding to the maximum possible quenching attainable.

$B=$	5×10^{4}	1×10^{5}	5×10^{5}	1×10^{6}	5×10^{6}	1×10^{7}	5×10^{7}	1×10^{8}	5×10^{8}	∞
$(\gamma+F)L^2(6D)^{-1}$										
1.0×10^{-2}	0.210	0.117	0.0259	0.0131	0.00265	0.00133	0.266×10^{-3}	0.133×10^{-3}	0.266×10^{-4}	0
3.0×10^{-2}	0.444	0.285	0.0739	0.0384	0.00791	0.00397	0.797×10^{-3}	0.399×10^{-3}	0.798×10^{-4}	0
5.0×10^{-2}	0.571	0.399	0.117	0.0623	0.0131	0.00660	0.00133	0.664×10^{-3}	0.133×10^{-3}	0
7.0×10^{-2}	0.650	0.482	0.157	0.0851	0.0183	0.00922	0.00186	0.930×10^{-3}	0.186×10^{-3}	0
1.0×10^{-1}	0.727	0.571	0.210	0.117	0.0259	0.0131	0.00265	0.00133	0.266×10^{-3}	0
2.5×10^{-1}	0.869	0.769	0.399	0.249	0.0623	0.0322	0.00660	0.00331	0.664×10^{-3}	0
5.0×10^{-1}	0.930	0.869	0.571	0.399	0.117	0.0623	0.0131	0.00660	0.00133	0
7.5×10^{-1}	0.952	0.909	0.666	0.499	0.166	0.0907	0.0196	0.00987	0.00199	0
1.0	0.964	0.930	0.727	0.571	0.210	0.117	0.0259	0.0131	0.00265	0
4.0	0.991	0.982	0.914	0.842	0.515	0.347	0.0961	0.0505	0.0105	0
7.0	0.995	0.989	0.949	0.903	0.650	0.482	0.157	0.0851	0.0183	0
1.0×10^{1}	0.996	0.993	0.964	0.930	0.727	0.571	0.210	0.117	0.0259	0
3.0×10^{1}	0.999	0.997	0.988	0.976	0.889	0.800	0.444	0.285	0.0739	0
5.0×10^{1}	0.999	0.998	0.993	0.985	0.930	0.869	0.571	0.399	0.117	0
1.0×10^{2}	1	0.999	0.996	0.993	0.964	0.930	0.727	0.571	0.210	0
4.0×10^{2}	1	1	0.999	0.998	0.991	0.982	0.914	0.842	0.515	0

nificantly from the behavior without it. The transient behavior of systems subject to excitation by time dependent sources can be calculated from Eq. (I-68).

IV. DISCUSSION

The results which we have obtained are encouraging and seem to justify an effort to establish the experimental use of fast reactions to study chain relaxation. From an experimental standpoint, the luminescence quenching studies seem to be the most promising in terms of feasibility. The possibility of making such measurements may be inferred from the work reviewed by Nishijima.[15] In addition, the effect of intramolecular interactions has been inferred,[16] and the possibility of synthesizing polymers with opposing ends terminated by fluorescing and quenching groups has also been suggested.[17]

With regard to the transient rate processes, one of the more significant experimental limitations might be the inability to obtain an equilibrium initial condition. The study of transients in luminescence quenching would be an effective way of surmounting this difficulty; however, other considerations indicate that this difficulty may not be of major importance. The slowest chain relaxation processes are governed by the relaxation frequency of the lowest normal mode, and this frequency is sufficiently greater than the decay constant characteristic of the long time behavior of the reacting system so that the absence of a well defined equilibrium initial condition might not be that serious. For example, for the ND chain we see from Table II for $\tau \approx 1$ that $\rho_L(1) \approx 0.09$, while from Table III we have $\phi(1) \approx \exp(-0.49)$ for the fastest reactions possible. This corresponds to there being about 61% of the end groups still unreacted for an initial *equilibrium* distribution. If the nonequilibrium starting condition had predominantly larger end-to-end separations than at equilibrium we might expect an even larger percentage of material to be unreacted when the relaxation to equilibrium was nearly complete.

The effect of different choices for s on ϕ and ν can be briefly mentioned. Provided s is an even function, no

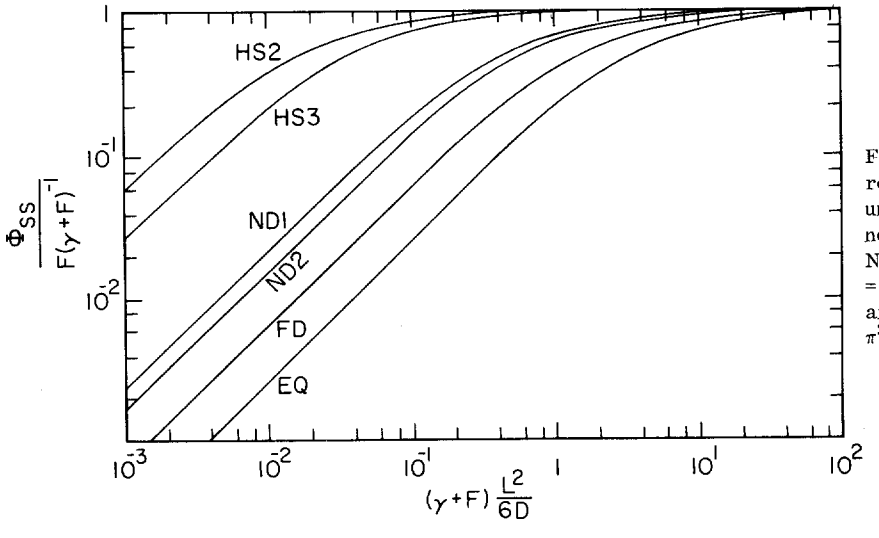

FIG. 3. Steady state luminescence quenching results for $B\gamma_R^3 = 5$. EQ: Maximum quenching under equilibrium conditions; FD: Free draining, no excluded volume forces. $\gamma_R = 0.01$; ND1: Nondraining, no excluded volume forces, $\gamma_R = 0.01$; ND2: Same as ND1, but $\gamma_R = 0.05$; HS2 and HS3: Harmonic spring with $\xi = 4.4082$ and π^2, and $\gamma_R = 0.01$.

qualitative changes in ϕ or ν will result. Even the time dependence of the higher terms in Eqs. (15) and (16) will be qualitatively correct since the chain relaxation frequencies which are shifted by the reaction to become the δ_i are determined solely by the evenness of s, not by its specific form, as was discussed in I. The actual values of the δ_i, ϕ_i, and ν_i, of course, depend quantitatively on the specific s function.

Finally, we note that the magnitudes of the various calculated quantities, e.g., k_1, ϕ_1, Φ_{ss}, seem reasonable from physical considerations, and that the results do have a very high degree of numerical self-consistency. Though it does not constitute a rigorous mathematical demonstration, this self-consistency lends credence to our supposition about the exponential character of $\phi(t)$ and $\nu(t)$. Specifically, we note that the integrals of ϕ and ν, the mean first passage time τ_m, and the luminescence quenching fraction Φ_{ss} can all be calculated independently of an assumed form for ϕ or ν, yet these quantities agree exceedingly well with those calculated on the basis of the exponential solution for ϕ.

ACKNOWLEDGMENTS

We would like to thank Dr. Andre Braun and Professor Harold Cassidy for suggesting this problem to us. Also, G. W. would like to acknowledge many helpful discussions with Dr. Harry Workman.

APPENDIX: CALCULATION OF EXPANSION COEFFICIENTS FOR $D(t)$

A. Harmonic spring model

For this simple model Eq. (I-142) defines the coefficient D_n. Using the Heaviside step function for s, Eq. (I-142) becomes

$$D_n = (4\pi R^3/3)^{-1}(2\pi L^2/3)^{-3/2}\int d\mathbf{r}\exp[-(3/2)(r/L)^2] \times H(R-r)h_n(\mathbf{r}). \quad \text{(A1)}$$

For $n=0$, $h_0(\mathbf{r})=1$, and with $\gamma_R=(3/2)^{1/2}(R/L)$ we obtain directly

$$D_0 = (4\pi R^3/3)^{-1}[\mathrm{erf}(\gamma_R) - (2/\pi^{1/2})\gamma_R\exp(-\gamma_R^2)]. \quad \text{(A2)}$$

Inspection of Eqs. (A1) and (I-A6)–(I-A9) shows that the smallest eigenvalue[18] λ_n for which the associated D_n is nonzero is

$$\lambda_{(1)} = 6DL^{-2}. \quad \text{(A3)}$$

The eigenfunctions[19] which contribute to the corresponding $D_{(1)}$ have the form $h_2(x)h_0(y)h_0(z)$. Thus $D_{(1)}$ is given as

$$D_{(1)} = (3/8)^{1/2}(4\pi R^3/3)^{-1}(2\pi L^2/3)^{-3/2} \times \int d\mathbf{r}\exp[-(3/2)(r/L)^2]H(R-r)H_2([3/2]^{1/2}[z/L]). \quad \text{(A4)}$$

The factor $3^{1/2}$ arises because there are three terms which make equal contributions to $D_{(1)}$ in Eq. (I-141). Since $H_2(u)=4u^2-2$ and $z=r\cos(\theta)$, Eq. (A4) can be reduced to

$$D_{(1)} = -(2/3)^{1/2}(4\pi R^3/3)^{-1}(2/\pi^{1/2})\gamma_R^3\exp(-\gamma_R^2). \quad \text{(A5)}$$

The next eigenvalue, $\lambda_{(2)}$, for which the associated coefficient is non-zero is

$$\lambda_{(2)} = 12DL^{-2}. \quad \text{(A6)}$$

The eigenfunctions which contribute to $D_{(2)}$ have the form

$$h_2(x)h_2(y)h_0(z)$$

or

$$h_4(x)h_0(y)h_0(z).$$

Thus we have

$$D_{(2)}^2 = (3/64)(4\pi R^3/3)^{-1}(\beta_1^2+\beta_2^2/6), \quad \text{(A7)}$$

where

$$\beta_1 = (2\pi L^2/3)^{-3/2}\int d\mathbf{r}\exp[-(3/2)(r/L)^2]H(R-r) \times H_2([3/2]^{1/2}[x/L])H_2([3/2]^{1/2}[z/L]) \quad \text{(A8)}$$

and

$$\beta_2 = (2\pi L^2/3)^{-3/2}\int d\mathbf{r}\exp[-(3/2)(r/L)^2]H(R-r) \times H_4([3/2]^{1/2}[z/L]). \quad \text{(A9)}$$

With $H_4(u)=16u^4-48u^2+12$, performing the integrals gives

$$\beta_1 = \beta_2/3 \quad \text{(A10)}$$

and

$$\beta_2 = (2/\pi^{1/2})8(\gamma_R^3 - 2\gamma_R^5/5)\exp(-\gamma_R^2), \quad \text{(A11)}$$

so

$$D_{(2)} = (10/(3\pi))^{1/2}(4\pi R^3/3)^{-1}(\gamma_R^3 - 2\gamma_R^5/5)\exp(-\gamma_R^2). \quad \text{(A12)}$$

The function $K(t)$ defined in Eq. (10) which results from the "unbalanced" choice of sinks is expressable as

$$K(t) = (4\pi R^3/3)(2\pi L^2/3)^{3/2}\lim_{R_1\to 0}\left[\sum_n D_n(R)D_n(R_1)\exp(-\lambda_n t)\right]. \quad \text{(A13)}$$

Taking this limit gives

$$K(t) = K_\infty + (2/\pi^{1/2})\gamma_R^3 e^{-\gamma_R^2}e^{-6DL^{-2}t} + (2/\pi^{1/2})(\tfrac{5}{4}\gamma_R^3 - \tfrac{1}{2}\gamma_R^5)e^{-\gamma_R^2}e^{-12DL^{-2}t} + \cdots. \quad \text{(A14)}$$

B. Chain model

From Eq. (I-117) in the $U=S^\alpha$ approximation we have

$$D(t) = v_{eq}^2 + \sum_{n\neq 0}\langle 0|s|n\rangle\langle n|s|0\rangle e^{-L_n t}. \quad \text{(A15)}$$

The smallest relaxation frequency, $L_{(1)}$, for which a nonzero coefficient is present in Eq. (A15) is

$$L_{(1)} = 2\Lambda_1. \quad \text{(A16)}$$

The appropriate members of the basis set have the form

$$|2_{1x},0,\cdots,0\rangle.$$

Thus,

$$D_{(1)} = 3^{1/2}\langle 0|s|2_{1x},0,\cdots,0\rangle \quad \text{(A17)}$$

which gives

$$D_{(1)} = (3/2)^{1/2}(4\pi R^3/3)^{-1}(2\pi)^{-3}\int d\mathbf{r}\,d\mathbf{k}\,H(R-r) \times \exp(-c_{ij}k^2 + i\mathbf{k}\cdot\mathbf{r})\langle 0|\exp(-i\mathbf{k}\cdot\mathbf{r}_*)$$

$$\times \exp(-i\mathbf{k}\cdot\mathbf{r}_-) b_{1x}^\dagger b_{1x}^\dagger |0\rangle \ , \qquad \text{(A18)}$$

upon using the Heaviside step function and Eqs. (I-89) and (I-90). After performing the required boson operator rearrangements[1] and the integral over **k**, the result is

$$D_{(1)} = (3/32)^{1/2} (f_1^2/c_{ij})(4\pi R^3/3)^{-1}(4\pi c_{ij})^{-3/2} \times \int d\mathbf{r} \exp[-r^2/(4c_{ij})] H(R-r) H_2(2^{-1}[x/c_{ij}]) \qquad \text{(A19)}$$

which is, of course, very similar to Eq. (A4). Finally, Eq. (A19) gives

$$D_{(1)} = -(2/3)^{1/2}(\pi f_1^2/c_{ij})(4\pi R^3/3)^{-1}(4\pi c_{ij}/R^2)^{-3/2} \times \exp[-R^2/(4c_{ij})] \ . \qquad \text{(A20)}$$

For a pair of groups on opposite ends of the chain Eqs. (A20), (I-16), and (I-18) give for $N \gg 1$

$$D_{(1)} = -(2^9/(3\pi^5))^{1/2}(4\pi R^3/3)^{-1}\gamma_R^3 \exp(-\gamma_R^2) \ . \qquad \text{(A21)}$$

From Eq. (A13), $K(t)$ may be obtained as

$$K(t) = K_\infty + (8/\pi^2)^2 (2/\pi^{1/2}) \gamma_R^3 e^{-\gamma_R^2} e^{-2A_1 t} + \cdots \ . \qquad \text{(A22)}$$

*Supported in part by NIH GM 13556 and by an NSF Predoctoral Fellowship, 1968-72, awarded to G. Wilemski.

†Based on a Ph.D. thesis submitted by G. Wilemski to the Graduate School of Yale University in 1972.

‡Present address: Department of Engineering and Applied Science, Yale University, New Haven, CT 06520.

[1]G. Wilemski and M. Fixman, J. Chem. Phys. **60**, 866 (1974), preceding article.

[2]Some recent articles on this subject include: K. Horie, I. Mita, and H. Kambe, Polymer J. **4**, 341 (1973); K. Ito, J. Polymer Sci. Part A-1 **10**, 3159 (1972); D. Peak, H. L. Frisch, and J. W. Corbett, Radiat. Eff. **11**, 149 (1971); D. Peak and J. W. Corbett, Phys. Rev. B **5**, 1226 (1972); W. Scheider, J. Phys. Chem. **76**, 349 (1972); K. S. Schmitz and J. M. Schurr, J. Phys. Chem. **76**, 534 (1972); G. Wilemski and M. Fixman, J. Chem. Phys. **58**, 4009 (1973). H. H. G. Jellinek, Polym. J. **4**, 489 (1973); J. M. Deutch and B. U. Felderhof, J. Chem. Phys. **59**, 1669 (1973); G. Czapski and E. Peled, J. Phys. Chem. **77**, 893 (1973). The bibliographies of these articles should be consulted for other examples.

[3]A. Horta and M. Fixman, J. Am. Chem. Soc. **90**, 3048 (1968).

[4]H. Yamakawa, *Modern Theory of Polymer Solutions* (Harper and Row, New York, 1971), pp. 272, 290.

[5]M. Fixman, J. Chem. Phys. **45**, 793 (1966).

[6]J. Boersma, Math. Comp. **14**, 380 (1960).

[7]Strictly there should be two straight lines, but by Eq. (14) (see accompanying remarks) BK_∞ is approximately constant for a wide range of γ_R. With the values of K_∞ listed in Table V it is easy to check that K_∞/γ_R^3 is constant to a very good approximation.

[8]G. Wilemski, Ph.D. thesis, Yale University (1972).

[9]In general, the threshold value of k will have some R and L dependence, decreasing as (R/L) decreases. For reactions of small molecules k is typically about 10^{10} liters (mole-sec)$^{-1}$ (1.66×10^{-11} cm^3/sec), but see A. M. North, Q. Rev. Chem. Soc. **20**, 421 (1966) for a variety of examples.

[10]For example: R. M. Noyes, Prog. React. Kinet. **1**, 129 (1961); T. R. Waite, Phys. Rev. **107**, 463 (1957).

[11]B. H. Zimm, J. Chem. Phys. **24**, 269 (1956); J. E. Hearst, J. Chem. Phys. **37**, 2547 (1962).

[12]M. Fixman, J. Chem. Phys. **45**, 785 (1966), Eqs. (93) and (95).

[13]P. H. Verdier, J. Chem. Phys. **45**, 2122 (1966).

[14]E. W. Montroll and K. E. Shuler, Advan. Chem. Phys. **1**, 361 (1958).

[15]Y. Nishijima, J. Polymer Sci. C. **31**, 353 (1970). See Refs. 41–47.

[16]E. P. Otocka, M. Y. Hellman, and L. L. Blyler, J. Appl. Phys. **40**, 4221 (1969).

[17]A. Braun and H. Cassidy (private communication).

[18]The symbol λ_n for the eigenvalues of the harmonic spring diffusion operator should not be confused with the Zimm–Hearst relaxation frequency λ_1.

[19]See the Appendix of Ref. 1 for the definition of the eigenfunctions.